Open Journal of Geology, 2026, 16(8), 451-469
https://www.scirp.org/journal/ojg
ISSN Online: 2161-7589
ISSN Print: 2161-7570

Landslide Susceptibility Mapping of the Kaushalya River Catchment, Solan, Himachal Pradesh, India: A Frequency Ratio Approach in a GIS Framework

Sonia Chhoker*, **Satish Kumar**, **Yoginder Singh**

Department of Geology, Kurukshetra University, Kurukshetra, Kurukshetra, India
Email: *sonia.chhoker95@kuk.ac.in

How to cite this paper: Chhoker, S., Kumar, S. and Singh, Y. (2026) Landslide Susceptibility Mapping of the Kaushalya River Catchment, Solan, Himachal Pradesh, India: A Frequency Ratio Approach in a GIS Framework. *Open Journal of Geology*, **16**, 451-469.
https://doi.org/10.4236/ojg.2026.168023

Received: June 2, 2026
Accepted: August 10, 2026
Published: August 13, 2026

Abstract

Landslide-affected roads are widespread within the Kaushalya River catchment, including the Pinjore-Dharampur stretch of NH-5, Kumharhatti-Nahan, Chakki Mod-Bhojnagar, and other link roads. A 30 m resolution Shuttle Radar Topography Mission (SRTM) based Digital Elevation Model (DEM) was utilized to delineate the Kaushalya River catchment. Landslide Susceptibility Map (LSM) was prepared for the Kaushalya River catchment. The DEM was further processed to derive slope, aspect, elevation, terrain roughness index (TRI), and curvature. Other conditioning factors including geology, land use and land cover, distance to road, distance to stream, distance to fault, and rainfall, were examined using a field-verified inventory of 213 landslide incidents. This study applies the Frequency Ratio (FR) method by integrating 11 conditioning factors within a GIS framework to assess landslide susceptible zones using Prediction Rate (PR). The resulting susceptibility map classified the catchment into five zones: very low, low, moderate, high, and very high. Model validation using Receiver Operating Characteristic (ROC) curve analysis yielded an Area Under the Curve (AUC) value of 0.747, which predicts a very good accuracy of LSM. The findings offer spatially explicit hazard information to assist regional planners, transportation engineers, and disaster management agencies.

Keywords

Kaushalya River Catchment, Digital Elevation Model, Landslide Susceptibility Map

1. Introduction

One of the biggest geo-hazards in the world, slope instability, results in thousands of deaths and annual economic losses of several billion dollars [1] [2]. In mountainous areas, where steep slopes, intricate geological settings, tectonic activity, and concentrated precipitation all contribute to the failure of hill slopes [3] [4]. The frequency and size of landslides have increased throughout the Himalayas in recent decades due to the combined effects of anthropogenic land-use pressure and climate-driven changes in rainfall characteristics, particularly rainfall intensity and duration [1] [2] [4]. The rough physiography, lithological heterogeneity, active tectonic framework, and strong monsoonal seasonality of the Indian Himalayan arc make it a very important setting in this regard [5]-[7]. Highway corridors have thus become areas of increased geohazard risk, which has significant effects on regional connectivity and economic continuity [8] [9]. Slope failures cause significant disruptions to transportation infrastructure, particularly highway networks that are vital to mountain towns, in addition to the immediate loss of life and property [10] [11]. Slope instability elevates the susceptibility of mass wasting and slope failure [12] [13]. These difficulties are faced along the Pinjore-Dharampur segment of National Highway-5 (NH-5) in Himachal Pradesh. The approximately 25-kilometer Pinjore-Dharampur road segment serves as a vital conduit for both passenger and commercial traffic between the Indo-Gangetic plains and the mid-Himalayan region. Statistical, probabilistic, and knowledge based methods have been used extensively to map the landslide vulnerable area along Himalayan highways. Several workers have developed landslide susceptibility maps by taking into account of various conditioning factors over the different segments of the Himachal Himalaya [11] [14]-[16]. These studies demonstrate the methodological foundation for FR-based susceptibility evaluation as well as the larger anthropogenic context in which slope instability along Himalayan highway has been exacerbated by road construction, slope modification lacking adequate geoscientific investigations, and shifting rainfall patterns.

The Pinjore-Dharampur road stretch had frequent landslides, rockfalls, and debris flows as a result of recent monsoon rains in 2024-2025. This resulted in significant disruption to the transportation infrastructure and frequent highway closures. In this quickly changing Himalayan environment, the reactivation of previously failed slopes during these occurrences emphasizes the growing role of intense rainfall in destabilizing already modified hillslopes. There are still few updated landslide susceptibility assessments for the Pinjore-Dharampur sector that specifically taken into account current geomorphological conditions and recent landslide inventory, notwithstanding these recent failures. In order to close this gap, the current study uses a GIS framework to conduct a thorough landslide susceptibility evaluation of the Kaushalya River catchment by the Frequency Ratio (FR) approach. Rapid infrastructure growth, highway widening, slope cutting, unplanned hill alteration, and poorly controlled construction techniques are the root cause of slope collapses in the Pinjore-Dharampur segment of NH-5 [8] [9] [15]. This study presents an updated GIS-based landslide susceptibility assessment of the Kaushalya River catchment using a recent landslide inventory that incorporates the impacts of the 2024-2025 monsoon events. The generated susceptibility map provides a scientific basis for identifying high-risk zones and supports sustainable highway planning and slope hazard mitigation along the Pinjore-Dharampur corridor.

2. Study Area

The study focused on the Kaushalya river catchment, including Dharampur-Pinjore section of NH-5 in Himachal Pradesh, India (**Figure 1**). The catchment covers 77˚01'28"E to 77˚05'00"E longitude and 30˚46'00"N to 30˚54'00"N latitude, located in Sub-Himalayan physiographic zone with altitudes ranging from 300 to 1500 meters above mean sea level (AMSL).The catchment is distinguished by rough ridge-valley topography, steep and heavily dissected hillslopes, and deeply incised stream channels formed by tectonic processes and fluvial erosion. Slopes range from smooth valley floors to extremely steep escarpments and road-cut walls. The region is drained by the Kaushalya River, a tributary of the Ghaggar River, while a network of seasonal streams cuts across the hill slopes and locally undercuts slope toes, increasing erosion and slope instability during the monsoon season. Geologically, the structurally complex portion of the Sub-Himalaya and is mostly underlain by Sirmur and Siwalik Group of rocks, including the Subathu, Dagshai, Kasauli Formations and Nahan and Pinjore Formations respectively. Along the NH-5, the Subathu, Dagshai, and Kasauli formations are exposed alternately, demonstrating significant tectonic juxtaposition and structural complexity [14].

The catchment have numerous thrusting zone and faults such as Jhajra Thrust (JT), Pinjore Garden Fault (PGF), Pinjore Thrust (PT), Bilaspur Thrust (BT) & Surajpur Thrust (ST), where the prominent thrusting zones are BT & ST. In BT, Subathu Formation thrusted over the Lower Siwalik group of rocks near the Parwanoo town, whereas the ST juxtaposes Subathu Formation over the Kasauli Formation in the vicinity of Chakki-mod. These conditions, combined with advanced weathering, extensive fracturing, jointing, and the presence of clay rich interlayers, diminish rock mass strength and promote the formation of crushed and shear zones, which are especially susceptible to slope collapse. The southwest monsoon has a considerable influence on the area's climate, which ranges from sub-tropical to sub-temperate. The average annual rainfall is 1413 mm, the most of which falls during the monsoon season. The Kaushalya catchment LULC is diverse, encompassing forested hillslopes, scrub covered slopes, farmed land, exposed bare surfaces, built-up areas, and highway infrastructure. In recent years, road widening, hill cutting, vegetation clearance, and the spread of towns and business facilities along NH-05 have altered natural slope geometry, increasing slope instability [15].

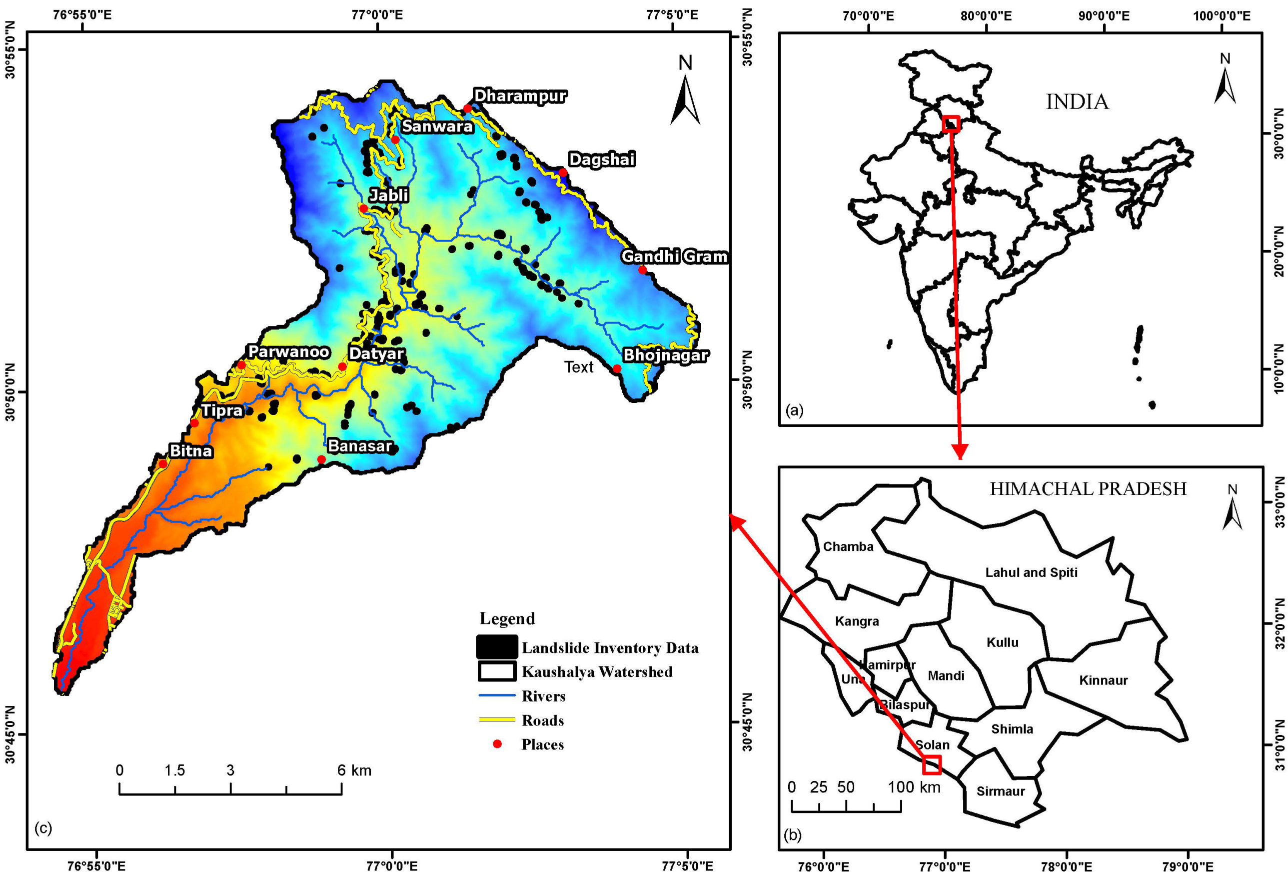

Figure 1. (a) (b) Inset maps of India and Himachal Pradesh are based on the Survey of India online map portal (https://surveyofindia.gov.in); (c) Location map of the Kaushalya River catchment along with relief, drainage and road network, derived from the SRTM 30 m DEM-catchment boundary, and landslide inventory was obtained from the National Geospatial Data Repository (https://geodataindia.gov.in/login).

3. Data & Methodology

The present study utilized multiple spatial datasets to derive the conditioning factors used in landslide susceptibility analysis. The Shuttle Radar Topography Mission (SRTM) based Digital Elevation Model (DEM) with a spatial resolution of 30 m, obtained (https://earthexplorer.usgs.gov/), and served as the principal topographic dataset for the study. The DEM was processed in a GIS environment to derive elevation based factors, including elevation, slope, aspect, curvature, and TRI. LULC data was obtained (https://livingatlas.arcgis.com/), prepared on Sentinel-2 imagery with a spatial resolution of 10 m. Fault, road, geology and stream datasets were accessed from the Bhukosh portal, governed by the Geological Survey of India (GSI). The integration of inventory data and thematic data of faults, roads and streams was processed to prepare distance to fault, distance to road, and distance to stream factor by Euclidean Distance tools in ArcGIS software. Daily rainfall data for the Kaushalya River catchment were obtained from the NASA Giovanni portal using the TRMM (Tropical Rainfall Measuring Mission) 3B42 Version 7 precipitation product for the period from 1 January 1998 to 30 November 2019. The TRMM 3B42 dataset provides precipitation estimates at a spatial resolution of 0.25˚ × 0.25˚ and was used to derive the rainfall conditioning factor for landslide susceptibility analysis. Data were collected from all thematic datasets were clipped to the study area boundary and prepared within a common GIS environment for subsequent analysis.

3.1. Landslide Inventory Preparation

A landslide inventory was created utilizing the landslide datasets made accessible through the GSI's Bhukosh Portal. The inventory was obtained in shapefile format and included 213 mapped landslide locations in the Kaushalya River watershed research area. Representative field photographs of documented landslide features are presented in Figure 2 and Figure 3. The inventory represents documented landslide events and was used as the dependent variable for landslide susceptibility modeling. The landslide locations were imported into the GIS system, verified for spatial consistency, and then used for model training and validation. A reliable landslide inventory is critical for susceptibility evaluation because it gives the spatial distribution of previous landslide events, which is used to build correlations between landslide incidence and the specified conditioning factors.

Figure 2. Field images of landslide features in the research region. (a) A small scale landslide with a visible escarpment indicating slope failure; (b) Rock mass instability with displaced boulders and imbalanced rock formations.

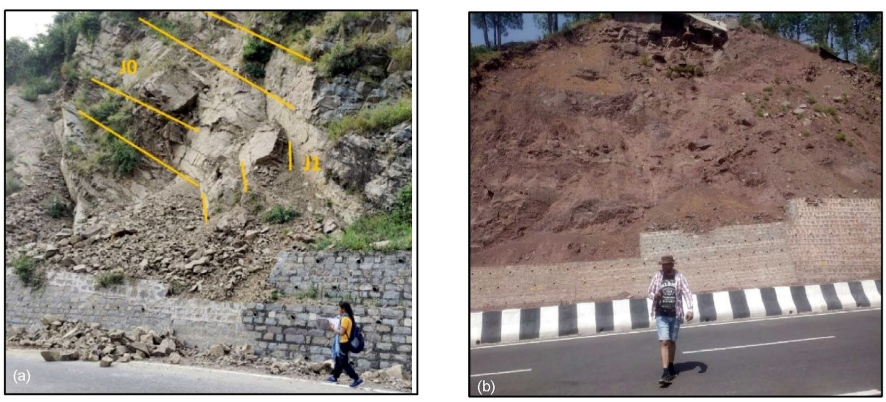

Figure 3. (a) Exposed bedrock demonstrating structural control through bedding plane dip direction and rockslide movement along weakness planes, and (b) a vulnerable residential building located in the path of an active landslide zone, emphasizing socioeconomic risk.

3.2. Conditioning Factor Preparation and Reclassification

The selection of conditioning factors is a pivotal step in any LSM exercise, as these variables collectively govern the mechanisms of slope failure initiation. Based on field observations, data availability, and previous landslide susceptibility studies in Himalayan terrain, 11 landslide conditioning factors were selected for the present analysis such as slope, aspect, curvature, rainfall, elevation, lithology, distance to roads, distance to streams, distance to faults, LULC and TRI. These factors were selected because they collectively represent the topographic, geological, hydrological, climatic, and anthropogenic controls, governed slope instability in the study area.

3.2.1. Slope

Slope gradient is widely recognized as the primary topographic determinant of landslide occurrence, directly governing gravitational shear stress and material resistance along slopes [17]. The slope map was extracted from the DEM using GIS and reclassified into five categories: 0˚ - 10˚, 10˚ - 20˚, 20˚ - 30˚, 30˚ - 40˚, and > 40˚. Steep gradients characterize the upper reaches and road cut sections, while gentler slopes are largely confined to valley floors and alluvial flats. Elevated landslide frequencies are generally associated with steeper slopes due to higher shear stress magnitudes, whereas gentle slopes typically remain stable in the absence of additional triggering mechanisms such as saturated lithologies, intense rainfall, or excavation.

3.2.2. Aspect

Slope aspect-the azimuthal direction a hillslope faces-exerts significant indirect control on landslide susceptibility through its modulation of microclimatic variables, including solar irradiation, evapotranspiration, soil moisture regime, vegetation density, and differential weathering intensity [18]. The aspect map was generated from the 30 m DEM using GIS tools, and continuous aspect values were reclassified into five directional classes based on predefined angular thresholds, corresponding to values 29, 130, 230, 331, and 431. This discretization facilitated systematic statistical evaluation of directional effects on landslide occurrence patterns.

3.2.3. Curvature

Terrain curvature describes the local concavity or convexity of the land surface and controls patterns of flow convergence/divergence and subsurface stress concentration [18]. Curvature was derived from the DEM and categorized into three classes: concave (-1), flat (0), and convex (+1). Concave slope forms exhibit higher frequencies of slope failure attributable to water accumulation and convergent sediment flux.

3.2.4. Rainfall

Precipitation is the foremost triggering factor for slope failures in the Himalayan context, operating primarily through pore-water pressure build-up and progressive reduction in effective soil shear strength [17]. Rainfall data from local meteorological stations were spatially interpolated using GIS-based techniques and classified into five zones with threshold values of 2.89, 2.99, 3.08, 3.18, and 3.28 cm. Zones receiving greater cumulative rainfall consistently exhibit higher landslide susceptibility indices.

3.2.5. Elevation

Elevation exerts a multifaceted influence on landslide susceptibility by modulating climatic gradients, orographic precipitation distribution, intensity of chemical weathering, soil profile development, and gravitational stress magnitudes [18] [19]. An elevation map derived from the 30 m DEM was classified into five altitudinal zones, with upper class boundaries at 668.46, 968.19, 1267.92, 1567.65, and 1867.38 m above mean sea level, enabling spatially uniform representation for statistical computation.

3.2.6. Lithology

Lithological characteristics govern landslide susceptibility through their influence on intact rock strength, hydraulic permeability, degree of weathering, and structural integrity [16] [18]. The lithological map was compiled from GSI geological sheets and processed in GIS. Six lithological units were delineated within the corridor: Dagshai, Siwalik, Kasauli, Dun region and terrace deposits, channel deposits, and Subathu Formation. Areal proportions are: Dagshai (42.34%), Subathu (24.22%), Kasauli (16.02%), Siwalik (8.91%), Dun and terrace (5.42%), and channel deposits (3.09%). Highly weathered and structurally weakened lithological units consistently demonstrate greater landslide susceptibility.

3.2.7. Distance to Streams

Proximity to drainage channels affects slope stability through processes of toe erosion, lateral bank undercutting, groundwater table fluctuations, and elevated pore-water pressures in adjacent materials [19]. The stream distance map was prepared from DEM-extracted drainage networks, and buffer zones at distances of 253.05 m, 532.74 m, 852.38 m, and 1698.11 m were delineated to assess the spatial extent of hydrological influence on landslide distribution.

3.2.8. Distance to Roads

Road proximity is a critical anthropogenic factor that amplifies landslide susceptibility through its associated impacts of slope undercutting, drainage modification, increased loading, and vibration from construction and traffic [16]. Euclidean distance analysis in GIS was applied to generate the distance-to-road, which was subsequently reclassified into four zones: 0 - 100 m, 100 - 200 m, 200 - 300 m, and > 300 m. Higher landslide densities are characteristically observed in the immediate proximity of road alignments.

3.2.9. Distance to Faults

Proximity to tectonic fault structures strongly conditions landslide susceptibility by creating zones of fractured, mechanically weakened rock and by concentrating seismically induced dynamic stresses [16] [18]. Euclidean distance from mapped fault traces was computed in GIS and classified into four categories: 0 - 500 m, 500 - 1000 m, 1000 - 1500 m, and 1500 - 2000 m.

3.2.10. LULC

Land use and land cover conditions modulate landslide processes through their effects on soil infiltration capacity, root reinforcement, surface runoff generation, and slope loading [16] [18]. The LULC map was generated from satellite imagery and categorized into four classes: water bodies, forested/tree-covered areas, bare soil, and built-up land. Forested areas dominate the corridor (70.88%), followed by built-up land (15.19%), soil cover (13.10%), and water bodies (0.83%). Built-up and exposed surfaces typically exhibit elevated susceptibility owing to slope modification and diminished vegetative protection.

3.2.11. TRI

Surface roughness is a proxy for topographic irregularity and captures the influence of relief heterogeneity on erosion potential, stress distribution, and hillslope hydrological behaviour [18] [20]. Roughness was derived from the DEM as the standard deviation of elevation within a focal moving window and classified into four categories: <1.75, 1.75 - 2.5, 2.5 - 3.25, and >3.25. Moderate roughness values (1.75 - 2.5) prevail across the largest proportion of the study area (49.35%), followed by low roughness (<1.75) at 48.40%, high roughness at 2.19%, and very high roughness at 0.05%.

3.3. Frequency Ratio (FR) Method

The Frequency Ratio method is a well-established bivariate statistical technique used to quantify the spatial association between past landslide occurrences and each conditioning factor class. Its application has been validated across a wide range of geological settings and terrain types. Mathematically, the FR for a given conditioning factor class is defined as the ratio of the proportional landslide occurrence within that class to the proportional area occupied by that class within the total study extent:

$$FR = \frac{\dfrac{N_{pix}(LX_i)}{\sum_{i=1}^{m} N_{pix}(LX_i)}}{\dfrac{N_{pix}(X_i)}{\sum_{i=1}^{m} N_{pix}(X_i)}} \tag{1}$$

where: FR = Frequency Ratio for class i; $N_{pix}(LX_i)$ number of landslide pixels within class i of the conditioning factor; $N_{pix}(X_i)$ = total number of pixels in class i; $N_{pix}(L)$ = total number of landslide pixels in the study area; $N_{pix}(X)$ = total number of pixels in the study area.

FR values exceeding 1.0 denote classes with above-average landslide propensity, while values below 1.0 indicate relatively stable conditions. To account for the differential predictive power of individual conditioning factors (1), FR values were normalized to Relative Frequency (RF) values on a 0 - 1 scale:

$$RF = \frac{FR_i}{\sum_{i=1}^{m} FR_i} \tag{2}$$

where, RF = Relative Frequency; FR_i = FR value of class i; m = total number of classes for that conditioning factor. The RF normalisation procedure follows [17].

Since RF normalization implicitly assigns equal weight to all conditioning factors (2), a Prediction Rate (PR) was computed for each factor using the training dataset to capture the differential contribution of each variable to landslide susceptibility:

$$PR = \frac{RF_{\max} - RF_{\min}}{(RF_{\max} - RF_{\min})_{\min}} \quad (3)$$

where, PR = Prediction Rate weight for the conditioning factor; $RF_{\max}$ = maximum RF value across all classes of that factor; $RF_{\min}$ = minimum RF value across all classes of that factor; $(RF_{\max} - RF_{\min})_{\min}$ = minimum RF range observed across all 11 conditioning factors, used as the normalisation denominator. The PR weighting procedure is adopted from Bonham-Carter (1994) [5] as applied by Li *et al.* (2017) [20].

Frequency Ratio (FR) Modelling

The Frequency Ratio (FR) method is a bivariate statistical approach that evaluates the spatial relationship between historical landslide occurrences and each class of the conditioning factors. For a given class of a conditioning factor, the FR value is computed as the ratio of the percentage of landslide pixels in that class to the percentage of the total area occupied by the same class. FR values greater than 1 indicate a positive association with landslide occurrence, whereas values less than 1 indicate relatively lower susceptibility. To standardize the influence of the factor classes, FR values were normalized into Relative Frequency (RF) values. In order to account for the differential contribution of individual conditioning factors, Prediction Rate (PR) values were subsequently calculated. The LSM was derived by integrating the RF values of the factor classes with their corresponding PR weights.

4. Results and Discussion

4.1. Frequency Ratio Analysis of Conditioning Factors

The Frequency Ratio (FR) model was used to assess the association between mapped landslides and the chosen landslide conditioning factors. **Table 1** shows the computed FR, RF, and PR values for the 11 conditioning factors. In general, FR > 1 implies that a specific class has a larger likelihood of landslide occurrence than the average condition in the research area, whereas FR < 1 indicates reasonably stable conditions. RF values describe the relative contribution of various classes, whereas PR values indicate the relative relevance of each conditioning element in determining the LSM. Among the examined parameters, slope angle had a substantial correlation with landslide occurrence.

The FR values gradually climbed from 0.14 for slopes < 10˚ to 0.62 for 10˚ - 20˚, 1.52 for 20˚ - 30˚, and a maximum of 3.44 for slopes 30˚ - 40˚ (**Figure 4(a)**). Although the FR value decreased significantly to 3.11 in slopes greater than 40˚, this class covers only a small portion of the watershed and is characterized by exposed competent bedrock with thin weathered cover (**Figure 4(b)**). The observed pattern indicates that moderately steep to steep slopes give the best circumstances for slope failure, as gravitational stress is considerable and worn material is readily available for mobilization. The PR value of 3.58 establishes slope gradient as a key regulating element in the Kaushalya catchment. The aspect factor showed relatively little variance, with FR values ranging from 0.72 to 1.24.

The 230˚ and 431˚ directional classes exhibited the most susceptibility. Although aspect is not an independent cause of slope failure, it does influence slope stability by regulating solar radiation, evapotranspiration, vegetation density, and soil moisture conditions. The relatively high PR value of 6.76 indicates that when combined with other topographic and environmental elements, this aspect contributes significantly to sensitivity.

Curvature (**Figure 4(c)**) showed very slight variations between the three classes. The convex class has the greatest FR value (1.12), while concave and flat surfaces had values close to one. This shows that curvature controls slope processes in a somewhat limited manner, primarily through its influence on runoff concentration, surface wash, and moisture redistribution, rather than functioning as a dominant regional driver. Rainfall (**Figure 4(d)**) had a moderate connection with landslide occurrences. The greatest FR value (0.32) was found in the 3.18 cm rainfall class, while the lowest rainfall class had no mapped landslide occurrence. Although the rainfall classes did not provide extremely high FR values, rainfall remained a major triggering factor in the research area because continuous monsoonal precipitation increases pore-water pressure, reduces shear strength, and destabilizes already weakened slopes. The PR value of 3.33 indicates the significance of rainfall when combined with topographic and geological circumstances. Elevation (**Figure 4(e)**) also had a significant effect on landslide distribution. The second elevation class had the highest FR value (2.10), followed by the third (1.13), while the lowest and highest elevation classes had FR values less than unity. This trend indicates that landslides are primarily concentrated in the medium elevation zones, where road construction, drainage incision, settlement growth, and weathered hill slopes are more prevalent. Elevation has an indirect impact on slope instability since it affects microclimate, vegetation, drainage conditions, and human activity levels. The PR value of 4.28 suggests a significant contribution to landslide occurrence.

Table 1. Frequency ratio (FR) and prediction rate (PR) values of landslide causative factors used in landslide susceptibility analysis.

Factors	Classes	Landslide Pixels%	Domain Pixels%	FR	RF	RF_{max}-RF_{min}	PR
Slope	<10˚	2.69	18.03	0.14	0.01	0.37	3.58
	10˚ - 20˚	25.27	40.93	0.62	0.07		
	20˚ - 30˚	53.23	35.55	1.52	0.17		
	30˚ - 40˚	18.28	5.30	3.44	0.38		
	>40˚	0.54	0.17	3.11	0.35		
	Sum			8.83	1		

Continued

Aspect	0˚ - 29˚	6.21	4.52	0.72	0.14		
	30˚ - 130˚	23.00	22.11	0.96	0.19		
	131˚ - 230˚	36.38	43.21	1.18	0.24		
	231˚ - 330˚	28.73	23.11	0.80	0.16		
	>331˚	5.66	7.03	1.24	0.25		
	Sum			4.92	1	0.10	6.76
Curvature	−1	19.23	19.09	0.99	0.33		
	0	31.01	25.12	0.81	0.27		
	>1	49.75	55.77	1.12	0.38		
	Sum			2.92	1	0.10	1.01
Rainfall(mm)	<2.90	5.52	0	0	0		
	2.91 - 2.99	22.19	16.58	0.22	0.23		
	3.00 - 3.08	24.78	31.15	0.24	0.26		
	3.09 - 3.18	32.88	35.67	0.32	0.34		
	3.19 - 3.28	14.60	16.58	0.14	0.15		
	Sum			0.94	1	0.34	3.33
Elevation(m)	<668	15.91	2.51	0.15	0.03		
	669 - 968	12.65	26.63	2.10	0.46		
	969 - 1267	31.37	35.67	1.13	0.25		
	1268 - 1567	34.97	34.67	0.99	0.22		
	1568 - 1867	5.07	0.50	0.09	0.02		
	Sum			4.48	1	0.44	4.28
Lithology	Dagshai Formation	42.33	39.11	0.92	0.19		
	Siwalik	8.91	5.77	0.64	0.13		
	Kasauli Formation	16.02	25.77	1.60	0.34		
	Piedmont	5.42	0	0	0		
	Terrace	0.39	0	0	0		
	Channel	3.08	0.88	0.28	0.06		
	Subhathu Formation	24.21	28.44	1.17	0.25		
	Sum			4.64	1	0.34	3.32
Distance to Stream	<253	35.76	50	1.39	0.42		
	253 - 532	30.31	33.33	1.09	0.33		
	532 - 852	23.59	14.51	0.61	0.18		
	>1698	10.32	2.15	0.20	0.06		
	Sum			3.32	1	0.36	3.43

Continued

Distance to Road	0 - 100	13.41	29.56	2.20	0.40		
	100 - 200	7.64	11.82	1.54	0.28		
	200 - 300	6.82	6.45	0.94	0.17		
	>300	72.11	52.15	0.72	0.13		
	Sum			5.42	1	0.27	2.61
Distance to fault	0 - 500	16.79	16.66	0.99	0.23		
	500 - 1000	17.11	24.73	1.44	0.33		
	1000 - 1500	15.67	16.12	1.02	0.23		
	1500 - 2000	50.41	42.47	0.84	0.19		
	Sum			4.30	1	0.13	1.33
LULC	Water body	0.82	0	0	0		
	Trees	70.87	84.94	1.19	0.53		
	Soil Cover	13.10	5.91	0.45	0.20		
	Built Up	15.19	9.13	0.60	0.26		
	Sum			2.25	1	0.53	5.10
Roughness	<1.75	48.40	18.59	0.38	0.02		
	1.75 - 2.5	49.34	69.34	1.40	0.08		
	2.5 - 3.25	2.19	11.55	5.27	0.32		
	>3.25	0.05	0.50	9.16	0.56		
	Sum			16.22	1	0.54	5.18

Lithology (**Figure 4(f)**) also has a significant impact on landslide occurrence. Lithological class 2 has the greatest FR value (1.60), followed by class 6 (1.17), while classes 1 and 5 had values below unity. One lithological unit had no mapped landslide occurrences. These variances represent differences in rock strength, weathering properties, structural discontinuities, permeability, and clay concentration between lithological units. Weak, worn, and heavily fractured sedimentary strata are more prone to slope failure, especially under heavy rains. The PR value of 3.32 demonstrates that lithology has an important role in the spatial distribution of landslides throughout the studied area. A clear inverse association was seen for distance to stream (**Figure 4(g)**).

The nearest stream buffer (≤253.05 m) had the greatest FR value (1.39), and FR values gradually dropped with increasing distance from drainage channels. This tendency suggests that slopes near streams are more prone to toe erosion, bank undercutting, saturation, and fluvial destabilization, all of which encourage landslide occurrence. The PR value of 3.43 emphasizes the importance of stream proximity in determining landslide distribution within the catchment. The distance to the road (**Figure 4(h)**) clearly demonstrates the anthropogenic influence on slope instability. Areas within 100 m of roadways had the highest FR value (2.20), followed by the 100 - 200 m class (1.54), while FR values dropped below unity beyond

300 m. This pattern demonstrates the destabilizing effect of road cutting, slope excavation, toe removal, blasting, and alteration of natural drainage pathways. The PR value of 2.62 indicates that road proximity is a significant human-caused factor influencing landslide activity in the Kaushalya River catchment. Distance to fault had a lesser influence than the other conditioning elements (**Figure 4(i)**). The greatest FR value (1.44) was recorded within the 500 - 1000 m buffer zone, while the remaining classes stayed near unity. This shows that fault-controlled zones may contribute to landslides by increasing fracture, weathering, and permeability, lowering rock-mass strength. However, in this study, fault proximity appears to have less influence than slope, terrain roughness, road proximity, and stream proximity.

LULC also had an impact on landslide occurrence with low PR value of 1.33 (**Figure 4(j)**). Forested areas had the highest FR value (1.19), while built-up land and bare soil had lower FR values of 0.60 and 0.45, respectively. There were no mapped landslides within bodies of water. Although vegetation is often thought to promote slope stability through root reinforcement and rainwater interception, in the current study, wooded regions are primarily found on steep natural hill slopes, where terrain characteristics are naturally prone to collapse. As a result, the observed association is more likely to represent the geomorphic setting of forest cover than the destabilizing influence of vegetation itself. The PR value of 5.10 indicates that LULC plays a substantial role when combined with terrain and lithological conditions.

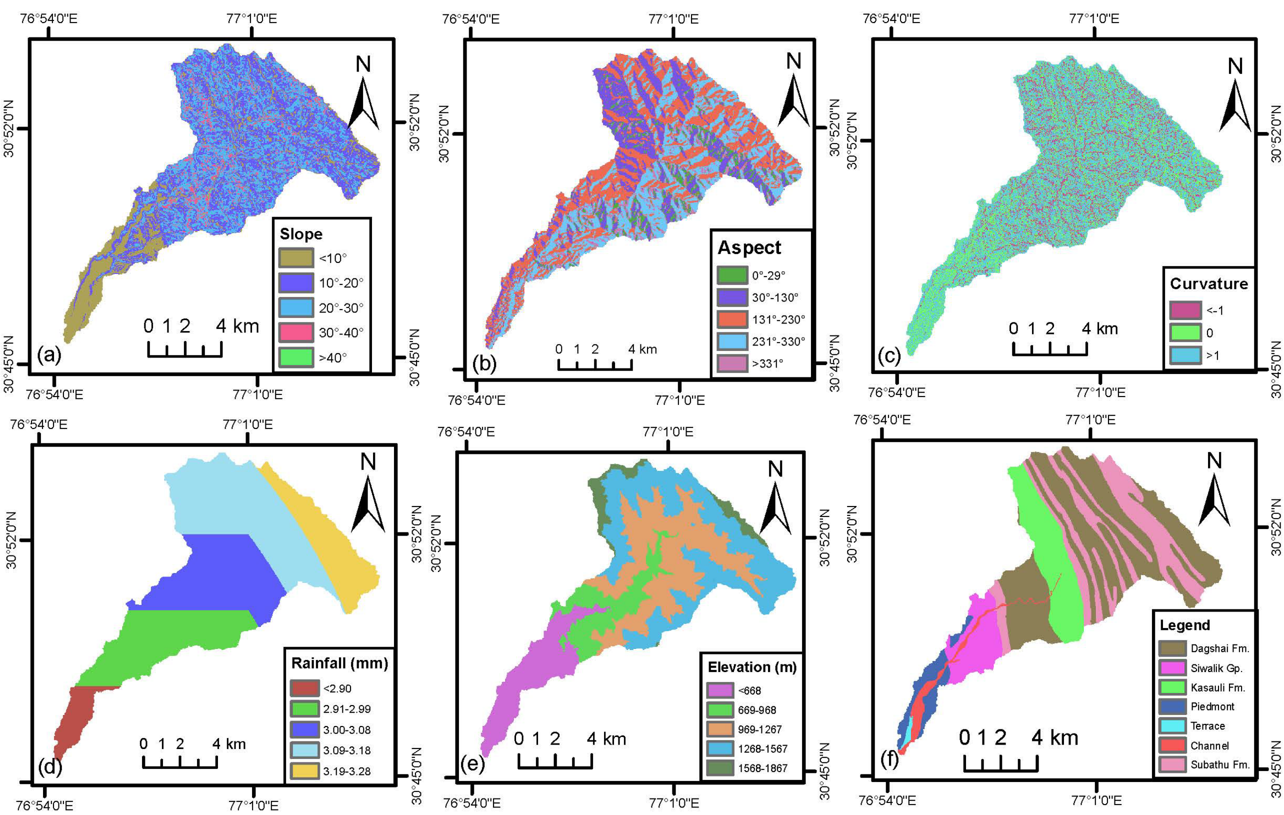

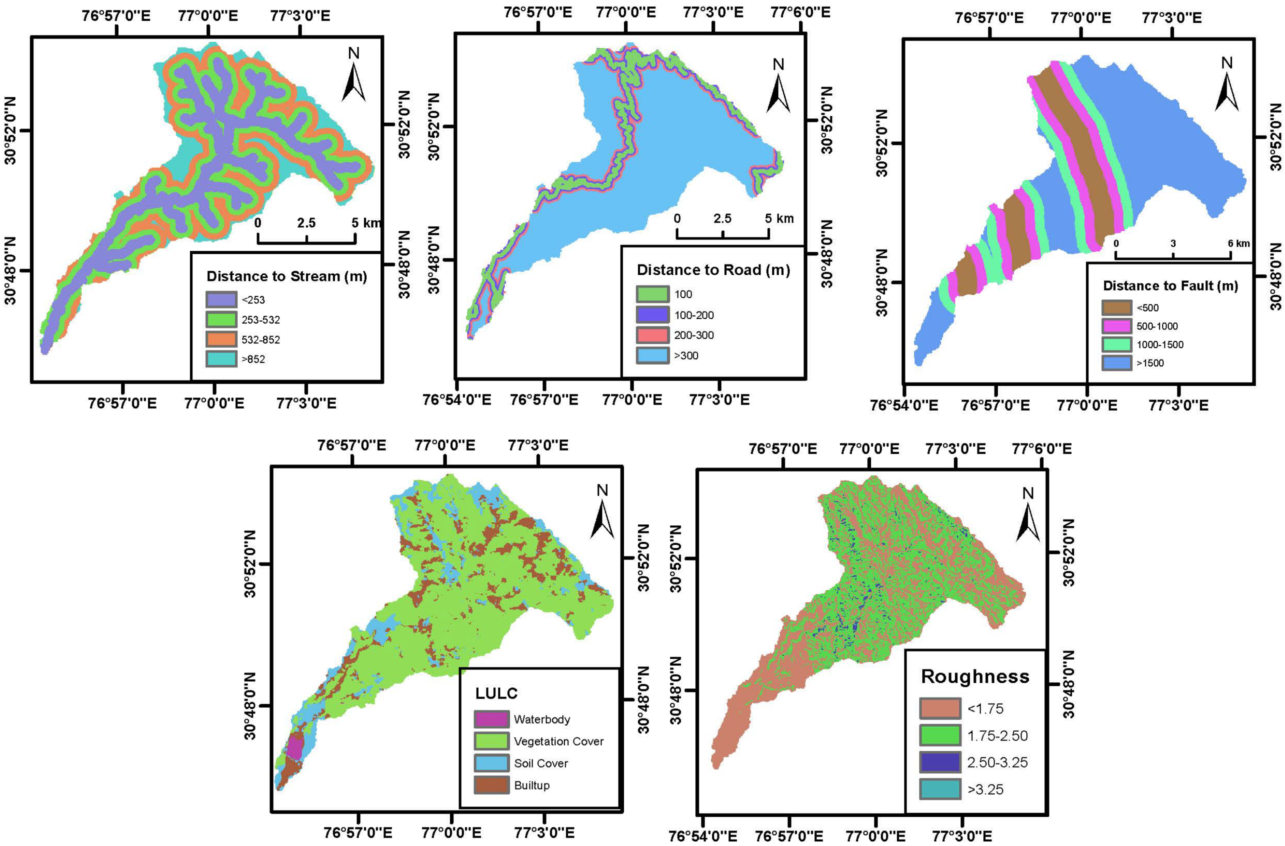

Figure 4. Thematic maps of the causative elements utilized in the landslide susceptibility analysis, including: (a) Slope; (b) Aspect; (c) Curvature; (d) Rainfall; (e) Elevation; (f) Lithology; (g) Distance to stream; (h) Distance to Road; (i) Distance to fault; (j) Land Use Land Cover (LULC); (k) Roughness.

Terrain roughness index (TRI) (Figure 4(k)) emerged as one of the most important variables in the study. FR values rose rapidly from 0.38 in the smoothest terrain to 1.40, 5.27, and 9.16 in the toughest class. The related RF values grew significantly as terrain roughness increased. These findings suggest that severely rough and dissected terrain is much more prone to landslides than smoother ground. Rugged terrain is usually linked with steep slopes, uneven topography, fragmented rock masses, small drainage channels, and extensive erosion, all of which contribute to slope instability. The PR value of 5.18 indicates terrain roughness as a strong predictor of landslide occurrence in the watershed.

Overall, the Prediction Rate values show that aspect (6.76), terrain roughness (5.18), LULC (5.10), elevation (4.28), slope (3.58), distance to streams (3.43), rainfall (3.33), lithology (3.32), distance to roads (2.62), and distance to faults (1.33) all contribute to landslide occurrence in the Kaushalya catchment. The findings show that landslide activity in the study area is influenced by a complex combination of topographic, geological, hydrological, climatic, and anthropogenic factors, rather than any one variable operating independently.

4.2. Landslide Susceptibility Zonation

The weighted PR layers were combined to yield the LSM, which was divided into five susceptibility zones using the Jenks Natural Breaks classification method (Figure 5). The generated susceptibility map demonstrates significant regional diversity in landslide risk throughout the Kaushalya River catchment. Very high to moderate susceptibility zones are located in steep hillslopes, rugged terrain, road-cut portions, stream-incised valleys, and places with structurally weak lithological units. In contrast, very low to low susceptibility zones are typically associated with gentler slopes, smoother terrain, and reasonably stable geological conditions.

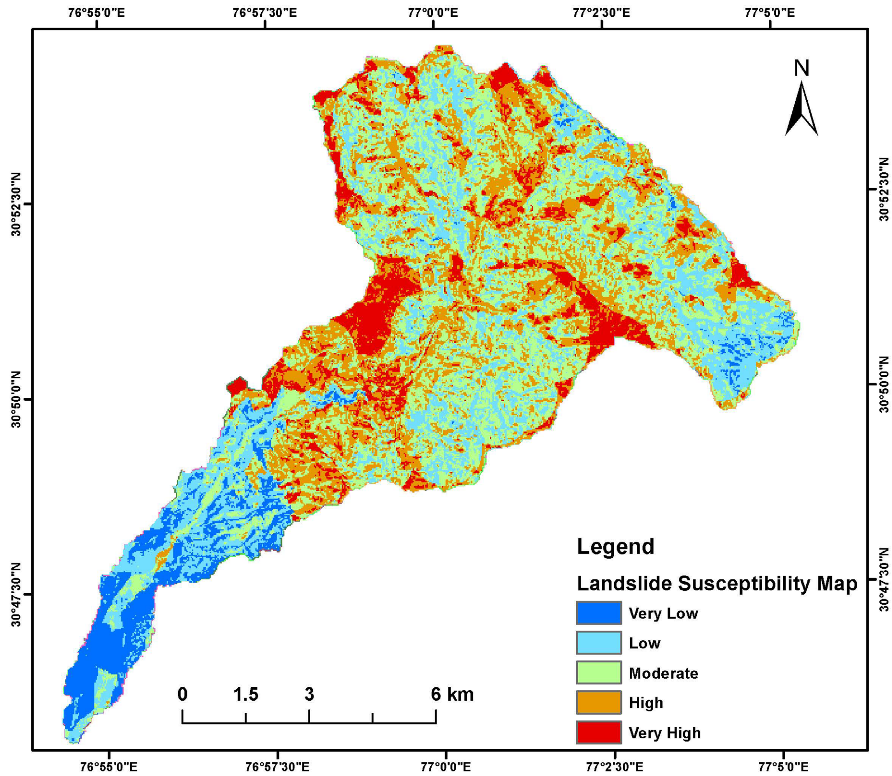

Figure 5. Landslide susceptibility map of the Pinjore-Dharmpur corridor with five susceptibility zones (very low, low, moderate, high, and very high) created using the Frequency Ratio approach.

The spatial pattern of susceptibility is consistent with the factor wise FR results and reflects the combined effects of slope gradient, terrain dissection, road closeness, stream erosion, lithological weakness, and monsoonal rainfall. The map thus gives a spatially explicit representation of landslide-prone terrain, which may be used to identify priority zones for slope stabilization and hazard mitigation.

4.3. Accuracy Assessment by ROC

A total of 213 mapped landslide polygons were used to validate the landslide susceptibility map (LSM). The polygon inventory was converted into point features in ArcGIS, and a 300 m buffer was generated around each landslide point. An equal number (213) of non-landslide points were then manually selected outside the buffered zones to represent the absence class. The resulting dataset of 426 presence–absence points was used for ROC analysis using Python. The predictive ability of the FR model was assessed using Receiver Operating Characteristic (ROC) analysis (Figure 6) The obtained AUC value of 0.747 shows very good prediction accuracy, implying that the chosen conditioning factors accurately describe the geographical pattern of landslide occurrence in the studied area. This level of model performance indicates that the resulting susceptibility map is dependable enough for landslide hazard assessment, infrastructure development, and disaster risk management in the Kaushalya River basin and the Pinjore-Dharmpur stretch of NH-5.

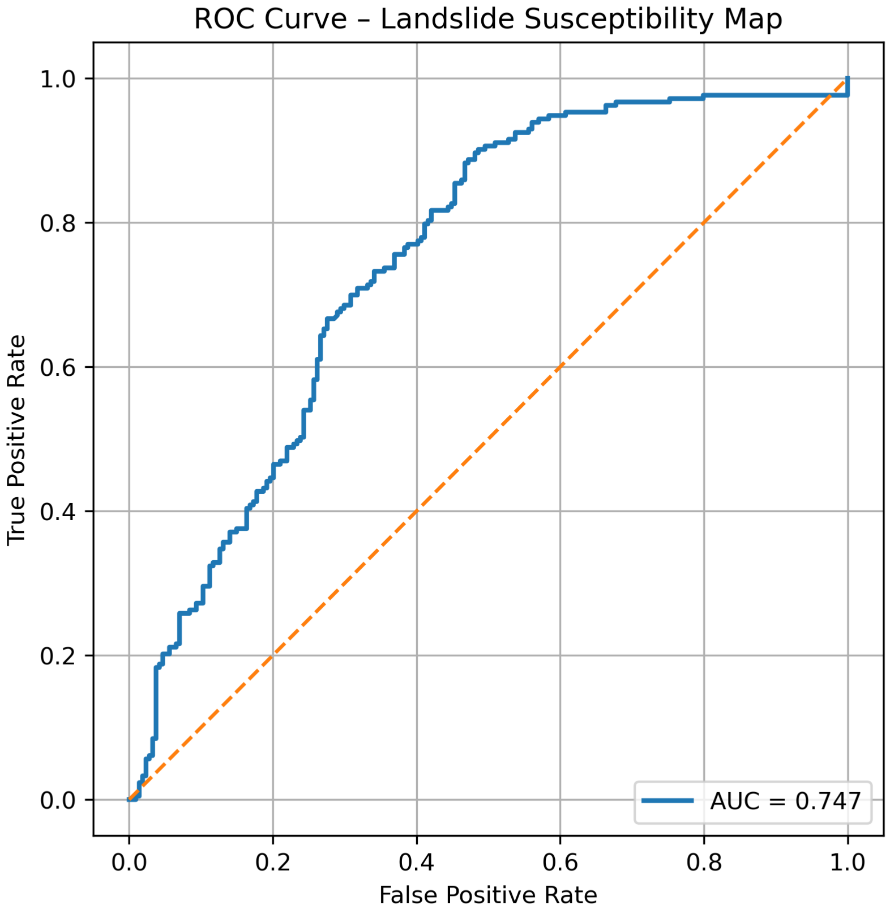

Figure 6. Receiver operating characteristic (ROC) curve illustrating the success rate and prediction rate of the landslide susceptibility model based on the Frequency Ratio approach.

5. Conclusions

The Kaushalya river catchment was assessed for landslide vulnerability using a GIS-based Frequency Ratio (FR) model. 11 topographic, geological, hydrological, climatic, structural, and anthropogenic conditioning elements were combined to create the LSM to identify landslide-prone area in the catchment.

The findings show that terrain, lithology, drainage, rainfall, and human disturbance all have an impact on landslide occurrence in the study area. Terrain roughness, slope gradient, elevation, proximity to fault, roads and streams, lithology, rainfall, and LULC were shown to be the most important constraints on landslide distribution, with aspect, curvature, and distance to faults having a very minor influence. High and extremely high susceptibility zones are primarily found on steep and rugged hillslopes, road cut portions, stream corridors, and places underlain by structurally weak and worn lithological formations.

The FR model had moderate to good predictive accuracy, with an AUC value of 0.747, showing that the selected conditioning factors adequately captured the geographical pattern of landslide incidence in the Kaushalya watershed. As a result, the created susceptibility map serves as a solid foundation for identifying hazard prone zones.

Areas in high and very high susceptibility zones should be prioritized for slope stabilization, better surface and subsurface drainage, bioengineering treatment, controlled slope cutting, and regular geotechnical monitoring. These enhancements would improve landslide risk assessment and lead to more resilient infrastructure planning in this landslide-prone Himalayan corridor.

Overall, the findings suggest that landslide incidence in the studied area is influenced by a combination of natural and anthropogenic factors. Steep slopes, harsh terrain, weak lithological units, closeness to roads and streams, and rainfall all contribute to slope failure. The resulting susceptibility map serves as a scientific foundation for identifying high risk zones, implementing slope-management methods, prioritizing the repair of susceptible road sections, and directing sustainable land use planning in this Himalayan catchment. The FR model was effective for regional scale susceptibility assessment, it could be improved further by incorporating higher resolution terrain and rainfall datasets, updating the landslide inventory, and using ensemble or machine learning approaches in future studies.

Author Contributions

Conceptualization: Ms. Sonia, Dr. Yoginder Singh;
Methodology: Ms. Sonia, Dr. Yoginder Singh;
Field Surveys and Data Collection: Ms. Sonia, Dr. Yoginder Singh;
Formal Analysis: Dr. Satish Kumar;
GIS Processing and Spatial Analysis: Ms. Sonia, Dr. Yoginder Singh;
Validation: Ms. Sonia, Dr. Satish Kumar, Dr. Yoginder Singh;
Writing—Original Draft Preparation: Ms. Sonia;
Writing—Review and Editing: Ms. Sonia, Dr. Satish Kumar, Dr. Yoginder Singh;
Visualization: Ms. Sonia, Dr. Yoginder Singh;
Supervision: Dr. Satish Kumar;
Project Administration: Ms. Sonia.

Conflicts of Interest

The authors declare no conflicts of interest regarding the publication of this paper.

References

[1] Ayalew, L., Yamagishi, H. and Ugawa, N. (2004) Landslide Susceptibility Mapping

Using GIS-Based Weighted Linear Combination, the Case in Tsugawa Area of Agano River, Niigata Prefecture, Japan. *Landslides*, **1**, 73-81. https://doi.org/10.1007/s10346-003-0006-9

[2] Akhtar, W., Siddique, T., Haris, P.M., Ahamad, A. and Mondal, M.E.A. (2023) An Integrated Geotechnical Study Using Q-Slope Method and Factor of Safety Appraisal along NH-5 from Solan to Shimla, India. *Journal of Earth System Science*, **132**, Article No. 106. https://doi.org/10.1007/s12040-023-02104-2

[3] Alsabhan, A.H., Singh, K., Sharma, A., Alam, S., Pandey, D.D., Rahman, S.A.S., *et al.* (2022) Landslide Susceptibility Assessment in the Himalayan Range Based along Kasauli-Parwanoo Road Corridor Using Weight of Evidence, Information Value, and Frequency Ratio. *Journal of King Saud University-Science*, **34**, Article ID: 101759. https://doi.org/10.1016/j.jksus.2021.101759

[4] Batar, A.K. and Watanabe, T. (2021) Landslide Susceptibility Mapping and Assessment Using Geospatial Platforms and Weights of Evidence (WoE) Method in the Indian Himalayan Region: Recent Developments, Gaps, and Future Directions. *ISPRS International Journal of Geo-Information*, **10**, Article No. 114. https://doi.org/10.3390/ijgi10030114

[5] Bonham-Carter, G.F. (1994) Geographic Information Systems for Geoscientists: Modelling with GIS. Pergamon.

[6] Chen, W., Pradhan, B., Li, S., Shahabi, H., Rizeei, H.M. and Hou, E. (2019) Novel Hybrid Integration Approach of Bagging-Based Fisher's Linear Discriminant Function for Landslide Susceptibility Mapping. *Geoscience Frontiers*, **10**, 1105-1116.

[7] Corominas, J., van Westen, C., Frattini, P., Cascini, L., Malet, J., Fotopoulou, S., *et al.* (2014) Recommendations for the Quantitative Analysis of Landslide Risk. *Bulletin of Engineering Geology and the Environment*, **73**, 209-263. https://doi.org/10.1007/s10064-013-0538-8

[8] Fawcett, T. (2006) An Introduction to ROC Analysis. *Pattern Recognition Letters*, **27**, 861-874. https://doi.org/10.1016/j.patrec.2005.10.010

[9] Froude, M.J. and Petley, D.N. (2018) Global Fatal Landslide Occurrence from 2004 to 2016. *Natural Hazards and Earth System Sciences*, **18**, 2161-2181. https://doi.org/10.5194/nhess-18-2161-2018

[10] Gautam, N. (2022) Landslide Susceptibility Mapping of Kinnaur District in Himachal Pradesh, India Using Probabilistic Frequency Ratio Model. *Journal of the Geological Society of India*, **98**, 1595-1604. https://doi.org/10.1007/s12594-022-2216-6

[11] Gupta, V. and Singh, K. (2023). Landslide Susceptibility Mapping along Chandigarh-Shimla Road Corridor NH-5, Himachal Pradesh, India. *AIP Conference Proceedings*, **2558**, Article ID: 020019. https://doi.org/10.1063/5.0130337

[12] Guzzetti, F., Mondini, A.C., Cardinali, M., Fiorucci, F., Santangelo, M. and Chang, K.-T. (2012) Landslide Inventory Maps: New Tools for an Old Problem. *Earth-Science Reviews*, **112**, 42-66. https://doi.org/10.1016/j.earscirev.2012.02.001

[13] Highland, L.M. and Bobrowsky, P. (2008) The Landslide Handbook—A Guide to Understanding Landslides. U.S. Geological Survey Circular 1325.

[14] Hong, H., Pradhan, B. and Xu, C. (2019) Spatial Prediction of Landslide Susceptibility Using Decision Tree-Based Machine Learning Techniques. *Catena*, **175**, 1-22.

[15] Sangeeta and Singh, S.K. (2023) Influence of Anthropogenic Activities on Landslide Susceptibility: A Case Study in Solan District, Himachal Pradesh, India. *Journal of Mountain Science*, **20**, 429-447. https://doi.org/10.1007/s11629-022-7593-1

[16] Kanungo, D.P., Arora, M.K., Sarkar, S. and Gupta, R.P. (2006) A Comparative Study of Conventional, ANN Black Box, Fuzzy and Combined Neural and Fuzzy Weighting Procedures for Landslide Susceptibility Zonation in Darjeeling Himalayas. *Engineering Geology*, **85**, 347-366. https://doi.org/10.1016/j.enggeo.2006.03.004

[17] Lee, S. and Sambath, T. (2006) Landslide Susceptibility Mapping in the Damrei Romel Area, Cambodia Using Frequency Ratio and Logistic Regression Models. *Environmental Geology*, **50**, 847-855. https://doi.org/10.1007/s00254-006-0256-7

[18] Lee, S. and Pradhan, B. (2007) Landslide Hazard Mapping at Selangor, Malaysia Using Frequency Ratio and Logistic Regression Models. *Landslides*, **4**, 33-41. https://doi.org/10.1007/s10346-006-0047-y

[19] Lee, S. and Talib, J.A. (2005) Probabilistic Landslide Susceptibility and Factor Effect Analysis. *Environmental Geology*, **47**, 982-990. https://doi.org/10.1007/s00254-005-1228-z

[20] Li, L., Lan, H., Guo, C., Zhang, Y., Li, Q. and Wu, Y. (2017) A Modified Frequency Ratio Method for Landslide Susceptibility Assessment. *Landslides*, **14**, 727-741. https://doi.org/10.1007/s10346-016-0771-x